Hindawi
Journal of Robotics
Volume 2019, Article ID 9531387, 10 pages
https://doi.org/10.1155/2019/9531387

Research Article

Construction and Layout of Coordinated Multirobots System Based on Parallel Thought

Wanqiang Xi,[1,2] Yaoyao Wang,[1] Yadong Ding,[1] and Bai Chen[1]

[1]*College of Mechanical and Electrical Engineering, Nanjing University of Aeronautics and Astronautics, Nanjing 210016, China*
[2]*College of Mechanical Engineering, Jiangsu University of Technology, Changzhou 213001, China*

Correspondence should be addressed to Yaoyao Wang; yywang_cmee@nuaa.edu.cn

Received 1 October 2018; Revised 4 December 2018; Accepted 19 December 2018; Published 3 January 2019

Academic Editor: Yangmin Li

Aiming at the problems that are the construction and the layout optimization of the coordinated multirobots system, the concept of an equivalent parallel robot (EPR) is proposed based on parallel thought in this paper. That is, each robot is regarded as a branched chain of the EPR in coordination. Thus, it can be converted into the problem for the type synthesis and the layout of the parallel robot. Firstly, the definition of robotic characteristic (C) set and the corresponding operational rule are given. Then, the minimum occupied area, cycle time, and condition number are used as the optimized objectives. The weight ratio is used to express the importance of the three objectives to meet the requirements of different scenes. Afterwards, based on the theory of C set, the three translational ($3T$) operational requirements that can be extended to other degree of freedom (DOF) are analyzed. Finally, the feasibility of the proposed methods is verified by the DOF analysis and simulation experiment. Moreover, the multiobjective layout problem is optimized based on the artificial bee colony (ABC) algorithm. The results show that the constructed robot combinations and the layout optimization method are satisfactory.

1. Introduction

The development of robotics has continuously improved the work capabilities of robots, and the field of robotic applications is constantly expanding [1, 2], for example, assembly work in automated factories, deep-sea operations, fault handling in the nuclear industry, and operational tasks in space. On the one hand, due to the complexity of the task, when a single robot is difficult to complete the task, people hope to accomplish this through coordination of multirobots [3]. On the other hand, people also hope to improve the efficiency of the robots system during the operation through the coordination of the multirobots [4]. Furthermore, when the working environment changes or the partial system fails, multirobots can still accomplish their scheduled tasks through their own fault tolerance [5]. In conclusion, compared with a single robot, multirobots system has higher stiffness, accuracy, load capacity, and flexibility [6, 7].

As a new form of robotic application, the coordinated multirobots have increasingly attracted the interest and concern of academic both at home and abroad. For the different operational tasks, different DOF may be required, so the robots need to be chosen to meet the operational DOF. Although the combinations of robots can meet the operational requirements, the unreasonable layout may reduce the efficiency of the system, occupy more areas, and have poor motion performance [8–10]. The previous work of the authors has done some research on the type synthesis of the coordinated multirobots system [11]. However, the C set in the description of the position and posture of a robot is not detailed enough, and the layout optimization is still lacking, and it cannot constitute the overall design of the coordinated multirobots system. These problems will be studied in this paper.

The layout of the multirobots system is to optimize its layout position according to different operational tasks after the branched robots are determined. The positions of the branched robots are adjusted for the different requirements of the task to achieve the best layout effect. However, for a parallel robot, it is generally achieved through dimension

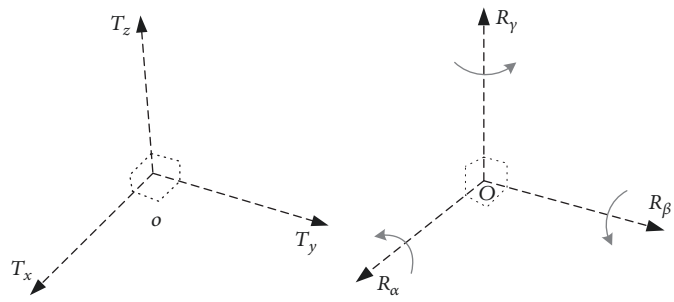

(a) Transnational features (b) Rotational features

Figure 1: Description for the end-features of the C set.

synthesis to meet the operational requirements; thus its branches will not change once they are laid out. At present, there are few relevant literatures on the layout of coordinated multirobots system. It mainly depends on the actual experience and cannot achieve the best results. Michele Gadaleta et al. proposed the method for the energy-optimal layout design of robotic work cells, which numerically retrieved the industrial robot base position to achieve the minimum energy consumption [12]. Zhen Yang Lim et al. presented a layout optimization method for multirobots cellular manufacturing system and compared the effects of several algorithms on the optimization results [13, 14]. However, either the optimized objectives are too single or the result of optimization is only an approximate areas. It is not possible to give an accurate layout according to the different operational tasks and the importance of the optimized objectives. This paper proposes to use the minimum occupied area, cycle time, and condition number as the optimized objectives. The weight coefficient is used to express the importance of the three objectives to meet the requirements for different scenes of the tasks, and the artificial bee colony (ABC) algorithm is used to optimize the multiobjective layout problem.

The main contributions of this paper are as follows. (a) The problem for the construction and layout optimization of a coordinated multirobots system is transformed into the type synthesis and layout of a parallel mechanism based on the parallel thought. (b) The concept of C set is presented, which can conveniently represent the end kinematic features (for the robot selection of multirobots) and the position and posture of the robot. (c) The multiobjective layout optimization method with weighted ratios is proposed, and the minimum occupied area, cycle time, and condition number are used as the optimized objectives. The remainder of this paper is organized as follows. In Section 2, the basic concept of robotic C set is given and corresponding intersection rule is analyzed. In Section 3, the minimum occupied area, cycle time, and condition number are taken as optimized objectives for the layout. The selection and layout of a specific task ($3T$) are mainly designed in Section 4. Lastly, Section 5 draws the conclusion.

2. Characteristic Set and Its Intersection Rule

The characteristic (C) set is used to describe the end-feature of a mechanism and the position and the posture of its base [11], as shown in

$$C = \left(T_x \;\; T_y \;\; T_z;\;\; R_\alpha \;\; R_\beta \;\; R_\gamma\right) \tag{1}$$

where T_i $(i = x, y, z)$ represents the translational features of robot's end-effector in the direction of x, y, and z and the position of its base. R_j $(j = \alpha, \beta, \gamma)$ represents the rotational features and the posture of its base. They are just as shown in Figure 1.

The meaning of the numerical values of the C set's elements is described in the literature [11]. The following examples are illustrated.

For example, there is a four-DOF robot with two translational features in the x and y directions and two rotational features rotating around the x and y axes, which belongs to a $2T2R$ robot. If the world coordinate system is set as the base coordinate system of the robot, its C set can be written as $(\overline{0} \;\; \overline{0} \;\; 0;\; \overline{0} \;\; \overline{0} \;\; 0)$. If the position and posture of the robot's base coordinate system is not 0 relative to the world coordinate system (neither the coordinates nor the RPY angles are 0), its C set can be written as $\left(T_x \;\; T_y \;\; \widehat{T}_z;\;\; R_\alpha \;\; R_\beta \;\; \widehat{R}_\gamma\right)$.

The operation of C set includes intersection and union, and the intersection is suitable for parallel mechanism [15, 16]. It is can be defined in

$$C = C_1 \cap C_2 = \left(T_x \;\; T_y \;\; T_z;\;\; R_\alpha \;\; R_\beta \;\; R_\gamma\right) \tag{2}$$

where $\cap$ stands for the intersection operator.

3. Layout of Multirobots

The layout optimization of a coordinated multirobots system can be considered as a parallel robot whose branched chains' positions are changed to achieve the minimum occupied area, cycle time, and condition number.

3.1. Occupied Area. Reasonable layout will reduce the occupied area of the completely coordinated multirobots system in the workshop [13]. For a parallel robot, the objective can be seen as the minimum of the static platform area by changing

the position and the posture of its branches to meet the required tasks. The calculation method of the occupied area is that the graphic area formed by the plane where the base of each robot is located. Moreover, it can be calculated based on the value of each robot's C set.

3.2. Cycle Time. In order to be more efficient, the production shop requires less time for the whole process. Therefore, it takes minimal time for EPR to complete the task. The cycle time of the EPR is determined by its rotation angle and the maximum angular velocity. The following equations are specified.

Assume that the angular velocity of the jth joint of No.i robot is ω_i^j. In a cycle time T, the continuous rotation angle of the jth joint is $|\theta_i^j|$, and the time of the jth joint is

$$T_i^j = \frac{\left|\theta_i^j\right|}{\omega_i^j} \quad (i, j = 1, 2, \ldots, n) \tag{3}$$

However, the running time of each robot's joint may be different. Now set the running time of No.i robot in the cycle time T as

$$T_i = \max\left(T_i^j\right) \tag{4}$$

During the cycle time T, the simultaneous tasks run for

$$T_s = \max\left(T_i\right) \quad (s = 1, 2, \ldots n) \tag{5}$$

Therefore, the total cycle time is the sum of the time for each independent task; that is,

$$T = \sum_{s=1}^{n} T_s \tag{6}$$

Similar to the EPR, it is required to arrange the position and the posture of each branch for a parallel robot reasonably. When the task is completed, the branch with the longest consumption time is considered as the minimum cycle time T of the parallel robot. In the following sections, the specific example will be given.

3.3. Condition Number. For serial robots, the statics performance index of robot's flexibility is generally used by Yoshikawa's manipulability index [17]. That is,

$$w_j = \sqrt{\left|J\left(q\right) J^T\left(q\right)\right|} \tag{7}$$

where $J(q)$ is the Jacobian matrix of the robot and $J^T(q)$ is the inverse of the Jacobian matrix. However, for a parallel robot, the condition number is often used as its performance index [18]. In a highly coupled multirobots cooperative system, such as multirobots transporting, it can be seen as an EPR, and its condition number is [19]

$$\kappa\left(J\right) = \|J\| \left\|J^{-1}\right\| \tag{8}$$

where $\|J\|$ is the norm of the Jacobian matrix J and for the 2-norm, the condition number can be written as [20]

$$\kappa\left(J\right) = \frac{\sigma_{\max}}{\sigma_{\min}} \tag{9}$$

where $\sigma_{\max}$ and $\sigma_{\min}$ are the maximum and minimum singular values of the Jacobian matrix J, respectively, and the range of the condition number is $1 \le \kappa(J) \le \infty$.

When designing a parallel robot, the value of the condition number should be 1 as far as possible [21]. Because when $\kappa(J) = 1$, the singular values are equal, and the arm is in an isotropic configuration with the highest flexibility.

3.4. Weight Fitness. Layout optimization means that the reasonable layout is selected to meet the different requirements. In this paper, the minimum occupied area, cycle time, and condition number are taken as the optimized objectives of the layout. However, in actual situation, one or two combinations may be dominant. Therefore, the proportion of these three evaluation indicators is particularly important, and the weight ratio will be used to express the importance of the three indicators.

The fitness of the area is expressed as

$$fit_a = \frac{1}{1 + \left(S - S_{\min}\right)} \tag{10}$$

where S is the occupied area and $S_{\min}$ is the minimum occupied area. The fitness of the operation time is expressed as

$$fit_t = \frac{1}{1 + \left(T - T_{\min}\right)} \tag{11}$$

where T is the cycle operation time and $T_{\min}$ is the minimum cycle operation time. The fitness of condition number is expressed as

$$fit_c = \frac{1}{1 + \left(N - N_{\min}\right)} \tag{12}$$

where N represents the condition number of the coordinated multirobots system and $N_{\min}$ represents the minimum condition number.

According to different operational requirements, a reasonable weight ratio is designed to represent the importance of the system's indicators:

$$fit = afit_a + bfit_t + cfit_c \tag{13}$$

where a, b, and c are the weight coefficients and $a + b + c = 1$. Their values are determined by their importance. The more important a certain indicator is, the greater its weight coefficient is.

The values of $S_{\min}$, $T_{\min}$, and $N_{\min}$ in the above three equations are obtained by ignoring the other two indicators. For example, when $S_{\min}$ is calculated, only the area indicator is considered, and the requirement of the operation time and the condition number are abandoned, that is, in the case where $a = 1$, $b = 0$, and $c = 0$.

To optimize the above-mentioned three objectives, the following assumptions are needed:

(1) If there is a nonstatic robot in the system (the base can move), its maximum moving area is set as the static area.

Table 1: The combinations of the branched robots with $3T$ motion.

Chain1	Chain2	Chain3	Combinations	Structure
C_1^{3T}	C_2^{3T}	C_3^{3T}	$C_1^{3T} \cap C_2^{3T} \cap C_3^{3T}$	symmetry
		C_3^{3T1R}	$C_1^{3T} \cap C_2^{3T} \cap C_3^{3T1R}$	
		C_3^{3T2R}	$C_1^{3T} \cap C_2^{3T} \cap C_3^{3T2R}$	
		C_3^{3T3R}	$C_1^{3T} \cap C_2^{3T} \cap C_3^{3T3R}$	
	C_2^{3T1R}	C_3^{3T1R}	$C_1^{3T} \cap C_2^{3T1R} \cap C_3^{3T1R}$	
		C_3^{3T2R}	$C_1^{3T} \cap C_2^{3T1R} \cap C_3^{3T2R}$	asymmetry
		C_3^{3T3R}	$C_1^{3T} \cap C_2^{3T1R} \cap C_3^{3T3R}$	
	C_2^{3T2R}	C_3^{3T2R}	$C_1^{3T} \cap C_2^{3T2R} \cap C_3^{3T2R}$	
		C_3^{3T3R}	$C_1^{3T} \cap C_2^{3T2R} \cap C_3^{3T3R}$	
	C_2^{3T3R}	C_3^{3T3R}	$C_1^{3T} \cap C_2^{3T3R} \cap C_3^{3T3R}$	
C_1^{3T1R}	C_2^{3T1R}	C_3^{3T1R}	$C_1^{3T1R} \cap C_2^{3T1R} \cap C_3^{3T1R}$	symmetry
		C_3^{3T2R}	$C_1^{3T1R} \cap C_2^{3T1R} \cap C_3^{3T2R}$	
		C_3^{3T3R}	$C_1^{3T1R} \cap C_2^{3T1R} \cap C_3^{3T3R}$	asymmetry
	C_2^{3T2R}	C_3^{3T2R}	$C_1^{3T1R} \cap C_2^{3T2R} \cap C_3^{3T2R}$	
		C_3^{3T3R}	$C_1^{3T1R} \cap C_2^{3T2R} \cap C_3^{3T3R}$	
C_1^{3T2R}	C_2^{3T2R}	C_3^{3T2R}	$C_1^{3T2R} \cap C_2^{3T2R} \cap C_3^{3T2R}$	symmetry

(2) The moving point is set as the base coordinate point of the robot.

(3) Each joint runs at the maximum speed.

4. Case Study

For example, a procedure of a factory's production line needs to transport the goods with heavy or bulk from worktable A to worktable B (only involving the three-dimensional translation of the space). However, many small-load robots with the same or different types cannot complete this task alone. Considering the cost savings, no new heavy-load robot will be purchased. At this time, it is necessary to filter and reorganize the existing robots in the factory and build a coordinated multirobots handling system composed of multiple robots.

Next, the above-mentioned type synthesis method and weight multiobjective optimization method will be used in the chain selection and the layout design of the EPR separately.

4.1. The Selection of the 3T EPR's Chains. The C set of the $3T$ EPR's end-manipulator is expressed as follows:

$$C = \begin{pmatrix} T_x & T_y & T_z; & 0 & 0 & 0 \end{pmatrix} \tag{14}$$

The literature [11] shows that the C set of the EPR's end-manipulator is determined by

$$C = C_1 \cap C_2 \cap C_3 \tag{15}$$

where C_1, C_2, and C_3 are the C sets of the EPR's three-branched robots, respectively, and the C set of the branched robots can be expressed as

$$C = \begin{pmatrix} T_x & T_y & T_z; & 0 & 0 & 0 \end{pmatrix} \tag{16}$$

$$C = \begin{pmatrix} T_x & T_y & T_z; & R_\alpha & 0 & 0 \end{pmatrix} \tag{17}$$

$$C = \begin{pmatrix} T_x & T_y & T_z; & R_\alpha & R_\beta & 0 \end{pmatrix} \tag{18}$$

$$C = \begin{pmatrix} T_x & T_y & T_z; & R_\alpha & R_\beta & R_\gamma \end{pmatrix} \tag{19}$$

It can be seen from (15) that the C set of the $3T$ EPR can be obtained by the intersection of the C sets for the above three-branched robots. As seen in Table 1, there are sixteen combinations of the branched chains, and the intersections must satisfy (2).

The classification and the condition of the combinations from Table 1 are listed in Table 2. According to the Table 1, the intersection just as $C = \begin{pmatrix} T_x & T_y & T_z; & 0 & 0 & 0 \end{pmatrix}$ has fifteen combinations and the proper subset of intersection just as $C = \begin{pmatrix} T_x & T_y & T_z; & 0 & 0 & 0 \end{pmatrix}$ has 9 combinations.

Since each branched chain of EPR is an independent robot, it can be a parallel or serial robot. The common robots with 3 to 6 DOF are listed in Table 3.

Then the combinations of the robots are selected to meet the task requirements ($3T$), and the choice of this paper is the combination of $C_1^{3T} \cap C_2^{3T3R} \cap C_3^{3T3R}$. That is, a parallel robot 3-*PRRR* and two six DOF serial robots are used as the EPR's branched chains to transport the goods, as shown in Figure 2. The three pneumatic hands are fixed under the moving platform of the 3-*PRRR* and the end of the serial robots to transport triangular goods. In this process, the three hands contact the goods closely without any change in position and posture between them. At this moment, the goods can be seen as a moving platform for the EPR, and the three robots are taken as the three-branched chains for the EPR. The screw theory [22] is used to analyze the DOF of EPR in the Equations (20), (21), and (24).

As shown in Figure 2, the parallel robot 3-*PRRR* is composed of a moving platform and a static platform, which are connected by the same three-branched chains. It is not difficult to see that the kinematic screw system of the parallel robot 3-*PRRR* is

Table 2: Classification for the combinations of the branched robots.

Objectives	Combinations	Conditions
$C = \begin{pmatrix} T_x & T_y & T_z; & 0 & 0 & 0 \end{pmatrix}$	$C_1^{3T} \cap C_2^{3T} \cap C_3^{3T}$	No requirements
	$C_1^{3T} \cap C_2^{3T} \cap C_3^{3T1R}$	
	$C_1^{3T} \cap C_2^{3T} \cap C_3^{3T2R}$	
	$C_1^{3T} \cap C_2^{3T} \cap C_3^{3T3R}$	
	$C_1^{3T} \cap C_2^{3T1R} \cap C_3^{3T1R}$	
	$C_1^{3T} \cap C_2^{3T1R} \cap C_3^{3T2R}$	
	$C_1^{3T} \cap C_2^{3T1R} \cap C_3^{3T3R}$	
	$C_1^{3T} \cap C_2^{3T2R} \cap C_3^{3T2R}$	
	$C_1^{3T} \cap C_2^{3T2R} \cap C_3^{3T3R}$	
	$C_1^{3T} \cap C_2^{3T3R} \cap C_3^{3T3R}$	
Proper subset is $C = \begin{pmatrix} T_x & T_y & T_z; & 0 & 0 & 0 \end{pmatrix}$	$C_1^{3T1R} \cap C_2^{3T1R} \cap C_3^{3T1R}$	Two are $\perp$ in $R_{\alpha1}$, $R_{\alpha2}$ and $R_{\alpha3}$
	$C_1^{3T1R} \cap C_2^{3T1R} \cap C_3^{3T2R}$	Three $\parallel$ cannot appear in $R_{\alpha1}$, $R_{\alpha2}$, $R_{\alpha3}$ and $R_{\beta3}$
	$C_1^{3T1R} \cap C_2^{3T1R} \cap C_3^{3T3R}$	$R_{\alpha1} \perp R_{\alpha2}$
	$C_1^{3T1R} \cap C_2^{3T2R} \cap C_3^{3T2R}$	Three $\parallel$ cannot appear in $R_{\alpha1}$, $R_{\alpha2}$, $R_{\beta2}$, $R_{\alpha3}$ and $R_{\beta3}$
	$C_1^{3T1R} \cap C_2^{3T2R} \cap C_3^{3T3R}$	$R_{\alpha1} \perp R_{\alpha2}$ and $R_{\alpha1} \perp R_{\beta2}$
	$C_1^{3T1R} \cap C_2^{3T1R} \cap C_3^{3T1R}$	$R_{\alpha1} \parallel R_{\alpha2} \parallel R_{\alpha3}$
	$C_1^{3T1R} \cap C_2^{3T1R} \cap C_3^{3T2R}$	Three is $\parallel$ in $R_{\alpha1}$, $R_{\alpha2}$, $R_{\alpha3}$ and $R_{\beta3}$
	$C_1^{3T1R} \cap C_2^{3T1R} \cap C_3^{3T3R}$	$R_{\alpha1} \parallel R_{\alpha2}$
	$C_1^{3T1R} \cap C_2^{3T2R} \cap C_3^{3T2R}$	Three is $\parallel$ in $R_{\alpha1}$, $R_{\alpha2}$, $R_{\beta2}$, $R_{\alpha3}$ and $R_{\beta3}$
	$C_1^{3T1R} \cap C_2^{3T2R} \cap C_3^{3T3R}$	Two is $\parallel$ in $R_{\alpha1}$, $R_{\alpha2}$, $R_{\beta2}$
	$C_1^{3T1R} \cap C_2^{3T3R} \cap C_3^{3T3R}$	
	$C_1^{3T2R} \cap C_2^{3T2R} \cap C_3^{3T3R}$	No requirements
	$C_1^{3T2R} \cap C_2^{3T3R} \cap C_3^{3T3R}$	
	$C_1^{3T3R} \cap C_2^{3T3R} \cap C_3^{3T3R}$	

Table 3: Common robots with 3 to 6 DOF.

Branched chain	Category	Robots
C^{3T}	serial	$P_1P_2P_3$, $R_1R_2R_2$
	parallel	Delta, 3-*PRRR*, 3-*RPS*
C^{3T1R}	serial	$R_1R_2R_2R_3$
	parallel	4-PU_1U_2
C^{3T2R}	serial	$R_1R_2R_2R_3R_4$
	parallel	5-*RPUR*
C^{3T3R}	serial	Puma560 (6*R*)
	parallel	Stewart (6-*UPS*)

$$S_1 = \begin{pmatrix} 0 & 0 & 0; & 0 & 0 & 1 \end{pmatrix}$$
$$S_2 = \begin{pmatrix} 0 & 0 & 0; & 0 & 1 & 0 \end{pmatrix} \quad (20)$$
$$S_3 = \begin{pmatrix} 0 & 0 & 0; & 1 & 0 & 0 \end{pmatrix}$$

Its corresponding reciprocal screw is

$$S_1^r = \begin{pmatrix} 0 & 0 & 0; & 0 & 0 & 1 \end{pmatrix}$$
$$S_2^r = \begin{pmatrix} 0 & 0 & 0; & 0 & 1 & 0 \end{pmatrix} \quad (21)$$
$$S_3^r = \begin{pmatrix} 0 & 0 & 0; & 1 & 0 & 0 \end{pmatrix}$$

The C set of the parallel robot 3-*PRRR* can be written as (22). If the base coordinate system of 3-PRRR is set to the world coordinate system o-xyz, its C set can be expressed as (23).

$$C_1 = \begin{pmatrix} T_{x1} & T_{y1} & T_{z1}; & 0 & 0 & 0 \end{pmatrix} \quad (22)$$
$$C_1 = \begin{pmatrix} \overline{0} & \overline{0} & \overline{0}; & 0 & 0 & 0 \end{pmatrix} \quad (23)$$

Similarly, the kinematic screw system of the six DOF serial robot is

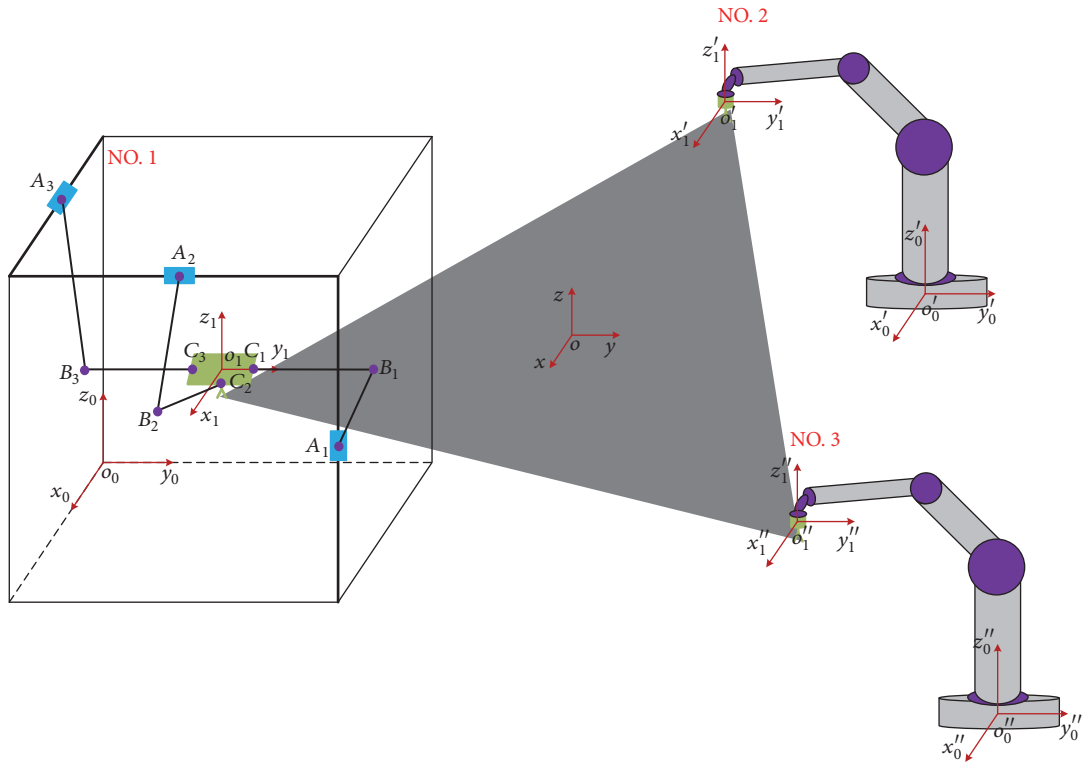

Figure 2: Three robots transporting triangular goods in coordination.

$$
\begin{aligned}
S_1 &= (1\ \ 0\ \ 0;\ \ 0\ \ 0\ \ 0)\\
S_2 &= (0\ \ 1\ \ 0;\ \ 0\ \ 0\ \ 0)\\
S_3 &= (0\ \ 0\ \ 1;\ \ 0\ \ 0\ \ 0)\\
S_4 &= (0\ \ 0\ \ 0;\ \ 1\ \ 0\ \ 0)\\
S_5 &= (0\ \ 0\ \ 0;\ \ 0\ \ 1\ \ 0)\\
S_6 &= (0\ \ 0\ \ 0;\ \ 0\ \ 0\ \ 1)
\end{aligned}
\tag{24}
$$

For a 6-DOF serial robot, it is obvious that the C set of its end kinematic features can be described as

$$
C_2 = (T_{x2}\ \ T_{y2}\ \ T_{z2};\ \ R_{\gamma 2}\ \ R_{\beta 2}\ \ R_{\alpha 2}) \tag{25}
$$

where the six elements are nonzero. According to (15), the end-features C set of EPR can be described as

$$
\begin{aligned}
C &= C_1 \cap C_2 \cap C_3\\
&= (T_{x1}\ \ T_{y1}\ \ T_{z1};\ \ 0\ \ 0\ \ 0)\\
&\quad \cap (T_{x2}\ \ T_{y2}\ \ T_{z2};\ \ R_{\gamma 2}\ \ R_{\beta 2}\ \ R_{\alpha 2})\\
&\quad \cap (T_{x3}\ \ T_{y3}\ \ T_{z3};\ \ R_{\gamma 3}\ \ R_{\beta 3}\ \ R_{\alpha 3})\\
&= (T_x\ \ T_y\ \ T_z;\ \ 0\ \ 0\ \ 0)
\end{aligned}
\tag{26}
$$

4.2. The Layout Design of the 3T EPR. When multirobots work in cooperative task, the layout will have a direct impact on the flexibility, operation time, and workspace of the multirobots system. Therefore, a reasonable layout is necessary. The method proposed in this paper is to use the minimum cycle time, occupied area, and condition number of the EPR as the optimized objectives, and their weight coefficients are chosen according to specific requirements.

As shown in Figure 2, the coordinate systems $o_0 - x_0y_0z_0$, $o_0' - x_0'y_0'z_0'$ and $o_0'' - x_0''y_0''z_0''$ are set to the base coordinates of No. 1, No. 2, and No. 3 robots, respectively. The Cartesian coordinate systems $o_1 - x_1y_1z_1$, $o_1' - x_1'y_1'z_1'$ and $o_1'' - x_1''y_1''z_1''$ are set to the moving coordinates of No. 1, No. 2, and No. 3 robots, respectively. $o - xyz$ is set to the coordinate system for the triangular goods, and $o_0 - x_0y_0z_0$ is also set to the world coordinate system of the EPR system. Assume that the starting coordinate A of the No.1 robot's manipulator is (0.2, 0.2, 0.3) and the ending coordinate B of its manipulator after the translation is (0.4, 0.4, 0.5). The DH parameters of the six DOF serial robot are listed in Table 4, and the corresponding coordinate systems of its linkages are shown in Figure 3.

The task requirement is to move the goods from point A to point B and optimize the layout of the EPR system with the minimum occupied area, cycle time, and condition number.

The coordinate system of the EPR system is established and the schematic diagram is shown in Figure 4. The circular modules with colors represent the base of the three robots, and the triangle modules represent the hands of the robots. The yellow pattern indicates the 3-*PRRR* parallel robot, and the green indicates the 6-DOF serial robot. The coordinate system of EPR system is projected onto the xy plane of the world coordinate system, and the coordinate of each module

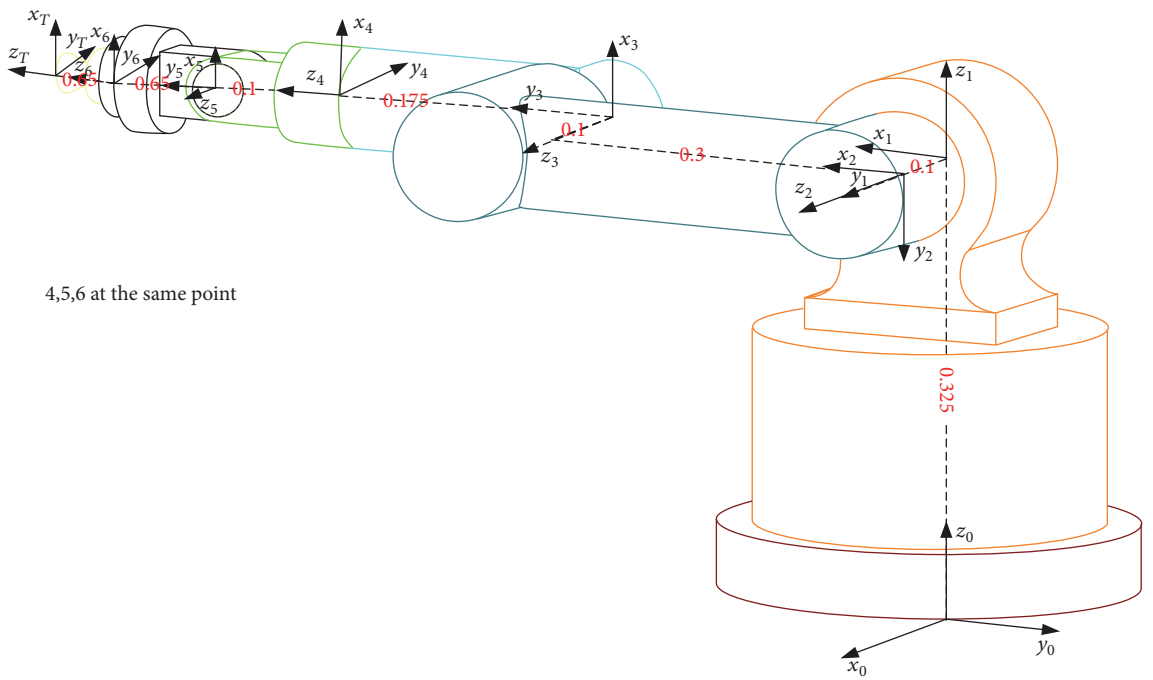

Figure 3: Six DOF serial robot links coordinate system.

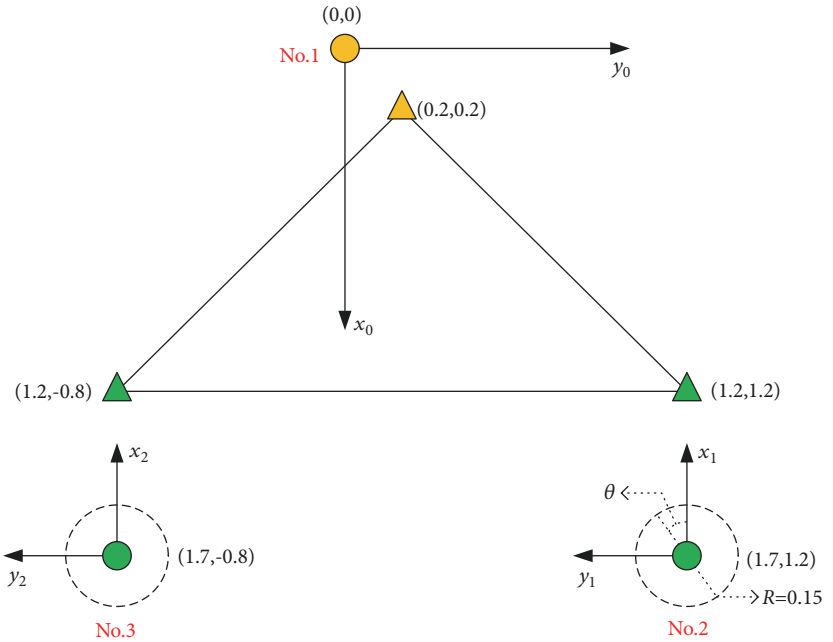

Figure 4: The coordinate systems diagram of the EPR layout.

Table 4: Six DOF serial robot parameters of links.

i	θ_i(rad)	d_i(m)	a_{i-1}(m)	α_{i-1}(rad)
1	$\theta_1(-\pi/2)$	0.325	0	0
2	0	0.1	0	$-\pi/2$
3	$\theta_3(-\pi/2)$	-0.1	0.300	0
4	0	0.405	0	$-\pi/2$
5	0	0	0	$\pi/2$
6	0	0	0	$-\pi/2$

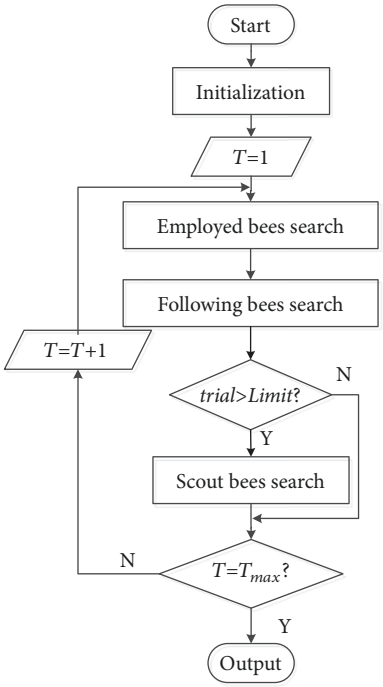

Figure 5: The flow chart of ABC algorithm.

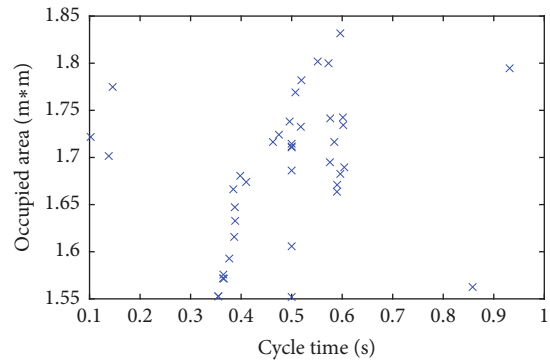

Figure 6: Scatter plot of cycle time and occupied area.

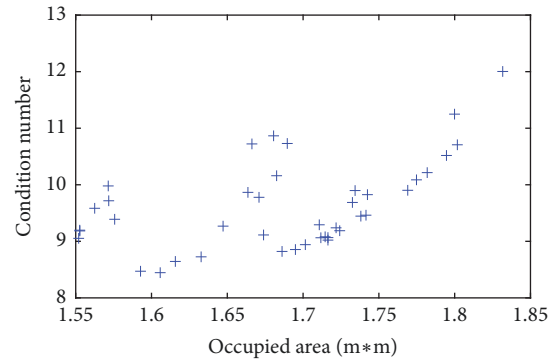

Figure 7: Scatter plot of occupied area and condition number.

is as shown in Figure 4. It is worth noting that, in the position layout of the robot, the base coordinate system of the fixed 3-*PRRR* is set as the world coordinate system, and only the positions of two six DOF serial robots can move.

The mathematical form of the three optimized objectives is described as follows:

$$\begin{aligned} \min \quad & y = f(R,\theta) = \left[f_s(R,\theta), f_t(R,\theta), f_c(R,\theta)\right] \\ s\,t \quad & 0 \le R \le 0.15 \\ & 0 \le \theta \le 2\pi \end{aligned} \tag{27}$$

where $f_s(R,\theta)$ represents the area optimized function. $f_t(R,\theta)$ represents the time optimized function. $f_c(R,\theta)$ represents the condition number optimized function. In addition, the circle of radius R and the rotation angle θ are the movable range of the serial robots.

The artificial bee colony (ABC) algorithm [23, 24] is used to optimize the multiobjective layout parameters, and its detailed procedure can be depicted in Figure 5. Since the EPR motion form belongs to the type of 3T, the two six-DOF serial robots (No. 2 and No. 3) keep the posture in the layout, as shown in Figure 4.

Assume that the maximum velocity of the parallel robot 3-*PRRR*'s prismatic joint is v=2.5m/s, the maximum velocity of the serial robot's rotational joint is ω=2πrad/s, and they run at the maximum velocity. Since the condition number of 3-*PRRR* is always 1 and the operation status of two serial robots is the same, the condition number of EPR is equivalent to the condition number of a serial robot. As long as the condition number of the serial robot is minimal, the condition number of EPR will be minimal.

Figures 6–8 show the plane distribution diagrams between cycle time, occupied area, and condition number. Figure 9 is a spatial distribution diagram of the three objectives set as spatial coordinate axes. The method of Monte Carlo is used to plot the diagrams in this paper. It can be seen that the scatter plots between the three objectives are not evenly distributed. The cycle time mainly concentrates on the range of 0.35 to 0.55, and the condition number mainly concentrates on the range of 8.5 to 11. In general, the condition number increases when the occupied area increases.

Different layout will affect the values of the three objectives, and it is particularly important to choose the layout location that meets the objective requirements. Next, the ABC algorithm will be used to search for the optimal solution according to the importance of its optimized objectives. The results obtained are shown in Table 5, and the corresponding C set of each branched robot in the EPR is shown in Table 6. When a=1, b=0, and c=0, the minimum occupied area $S_{\min}$=1.5500m^2 can be obtained. Similarly, when a=0, b=1, and c=0, the minimum cycle time $T_{\min}$=0.0903s, and when a=0, b=0, and c=1, the condition number $C_{\min}$=8.4253. As seen in Table 5, the values of the objectives decrease as the weight coefficient increases, which is consistent with the results of multiobjective optimization. From Table 6, the C sets of each group of branched robots represent their end kinematic features, the position, and the posture of their layout, which greatly facilitates the selection and layout of the multirobots.

Table 5: Optimization results with different weight coefficients.

Number	a	b	c	R	θ	area	time	condition
1	1	0	0	0.1500	0	1.5500	-	-
2	0.6	0.2	0.2	0.1283	5.8478	1.5837	0.1281	8.5469
3	0.33	0.34	0.33	0.1185	5.5168	1.6146	0.1154	8.4512
4	0.2	0.6	0.2	0.0773	0.2950	1.6260	0.1349	8.7242
5	0	1	0	0.1500	4.6911	-	0.0903	-
6	0.2	0.2	0.6	0.1263	5.7336	1.5923	0.1239	8.4776
7	0	0	1	0.1500	5.5328	-	-	8.4253

Table 6: The C set of each robot under different weight coefficients.

Number	No.1 (C)	No.2 (C)	No.3 (C)
1	$(\overline{0}\ \overline{0}\ \overline{0};\ 0\ 0\ 0)$	$(1.55\ \ 1.2\ \ \overline{0};\ \overline{0}\ \overline{0}\ \pi)$	$(1.55\ \ -0.8\ \ \overline{0};\ \overline{0}\ \overline{0}\ \pi)$
2	$(\overline{0}\ \overline{0}\ \overline{0};\ 0\ 0\ 0)$	$(1.5837\ \ 1.2541\ \ \overline{0};\ \overline{0}\ \overline{0}\ \pi)$	$(1.5837\ \ -0.7459\ \ \overline{0};\ \overline{0}\ \overline{0}\ \pi)$
3	$(\overline{0}\ \overline{0}\ \overline{0};\ 0\ 0\ 0)$	$(1.6146\ \ 1.2822\ \ \overline{0};\ \overline{0}\ \overline{0}\ \pi)$	$(1.6146\ \ -0.7178\ \ \overline{0};\ \overline{0}\ \overline{0}\ \pi)$
4	$(\overline{0}\ \overline{0}\ \overline{0};\ 0\ 0\ 0)$	$(1.6260\ \ 1.1775\ \ \overline{0};\ \overline{0}\ \overline{0}\ \pi)$	$(1.6260\ \ -0.8225\ \ \overline{0};\ \overline{0}\ \overline{0}\ \pi)$
5	$(\overline{0}\ \overline{0}\ \overline{0};\ 0\ 0\ 0)$	$(1.7032\ \ 1.35\ \ \overline{0};\ \overline{0}\ \overline{0}\ \pi)$	$(1.7932\ \ -0.65\ \ \overline{0};\ \overline{0}\ \overline{0}\ \pi)$
6	$(\overline{0}\ \overline{0}\ \overline{0};\ 0\ 0\ 0)$	$(1.5923\ \ 1.266\ \ \overline{0};\ \overline{0}\ \overline{0}\ \pi)$	$(1.5923\ \ -0.734\ \ \overline{0};\ \overline{0}\ \overline{0}\ \pi)$
7	$(\overline{0}\ \overline{0}\ \overline{0};\ 0\ 0\ 0)$	$(1.5903\ \ 1.3023\ \ \overline{0};\ \overline{0}\ \overline{0}\ \pi)$	$(1.5903\ \ -0.6977\ \ \overline{0};\ \overline{0}\ \overline{0}\ \pi)$

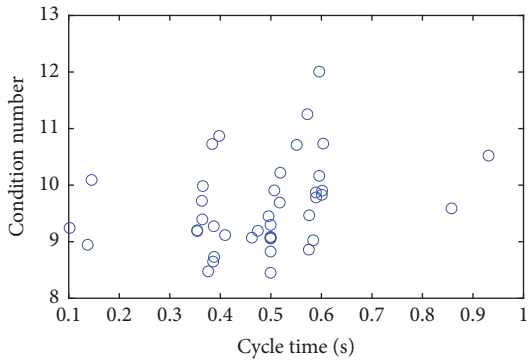

Figure 8: Scatter plot of cycle time and condition number.

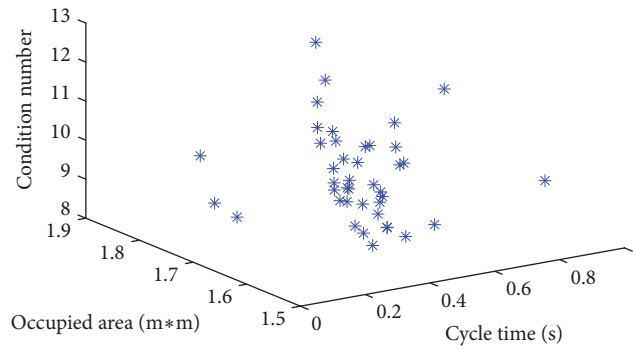

Figure 9: Scatter plot of cycle time, occupied area and condition number in the space.

5. Conclusions

In this paper, the concept of EPR is proposed based on the parallel thought. The problem for the construction and layout optimization of a coordinated multirobots system is transformed into the selection and layout of the branched chains of a parallel robot. Firstly, the concept of C set and its operational rule are presented, which can conveniently represent the end kinematic features and the position and posture of the robot. The selection scheme of EPR satisfying the requirements is constructed based on the intersection rule of the C set. After that, the ABC algorithm is used to optimize the selected robots according to the principle of minimum occupied area, cycle time, and condition number. Based on the importance of the three optimized objectives, a multiobjective optimization for the multirobots system with weighted ratios is proposed. The occupied area, cycle time, condition number, and the locations of the robots under different weight coefficient can be obtained by the simulation experiments. The results show that the proposed methods are feasible.

In future, the work may involve the selection and layout of multirobots in more complex situations. For example, consider the situations of more tasks, more operational sequences, and more robots.

Data Availability

No data were used to support this study.

Conflicts of Interest

The authors declare that there are no conflicts of interest regarding the publication of this paper.

Acknowledgments

This research was supported by the National Natural Science Foundation of China (Grants nos. 51575256, 51705243, and

51706098) and the Natural Science Foundation of Jiangsu Province (BK20170789).

References

[1] L. Ding, X. Li, Q. Li, and Y. Chao, "Nonlinear Friction and Dynamical Identification for a Robot Manipulator with Improved Cuckoo Search Algorithm," *Journal of Robotics*, vol. 2018, Article ID 8219123, 10 pages, 2018.

[2] M. Hosseini, R. Meattini, G. Palli, and C. Melchiorri, "A Wearable Robotic Device Based on Twisted String Actuation for Rehabilitation and Assistive Applications," *Journal of Robotics*, vol. 2017, Article ID 3036468, 11 pages, 2017.

[3] P. R. Culmer, A. E. Jackson, S. Makower et al., "A control strategy for upper limb robotic rehabilitation with a dual robot system," *IEEE/ASME Transactions on Mechatronics*, vol. 15, no. 4, pp. 575–585, 2010.

[4] S. Manzoor, S. Lee, and Y. Choi, "A Coordinated Navigation Strategy for Multi-Robots to Capture a Target Moving with Unknown Speed," *Journal of Intelligent & Robotic Systems*, vol. 87, no. 3-4, pp. 627–641, 2017.

[5] D.-H. Lee, H. Park, J.-H. Park, M.-H. Baeg, and J.-H. Bae, "Design of an anthropomorphic dual-arm robot with biologically inspired 8-DOF arms," *Intelligent Service Robotics*, vol. 10, no. 2, pp. 137–148, 2017.

[6] S. Erhart and S. Hirche, "Internal Force Analysis and Load Distribution for Cooperative Multi-Robot Manipulation," *IEEE Transactions on Robotics*, vol. 31, no. 5, pp. 1238–1243, 2015.

[7] W. Wan and K. Harada, "Developing and Comparing Single-Arm and Dual-Arm Regrasp," *IEEE Robotics & Automation Letters*, vol. 1, no. 1, pp. 243–250, 2016.

[8] S. Angra, R. Sehgal, and Z. Samsudeen Noori, "Cellular manufacturing-A time-based analysis to the layout problem," *International Journal of Production Economics*, vol. 112, no. 1, pp. 427–438, 2008.

[9] M. Pellicciari, G. Berselli, F. Leali, and A. Vergnano, "A method for reducing the energy consumption of pick-and-place industrial robots," *Mechatronics*, vol. 23, no. 3, pp. 326–334, 2013.

[10] I. Suemitsu, K. Izui, T. Yamada, S. Nishiwaki, A. Noda, and T. Nagatani, "Simultaneous optimization of layout and task schedule for robotic cellular manufacturing systems," *Computers & Industrial Engineering*, vol. 102, pp. 396–407, 2016.

[11] W. Xi, B. Chen, Y. Wang, and F. Ju, "Type synthesis of coordinated multi-robot system based on parallel thought," *Transactions of the Canadian Society for Mechanical Engineering*, vol. 42, no. 2, pp. 164–176, 2018.

[12] M. Gadaleta, G. Berselli, and M. Pellicciari, "Energy-optimal layout design of robotic work cells: Potential assessment on an industrial case study," *Robotics and Computer-Integrated Manufacturing*, vol. 47, pp. 102–111, 2017.

[13] Z. Y. Lim, S. G. Ponnambalam, and K. Izui, "Multi-objective hybrid algorithms for layout optimization in multi-robot cellular manufacturing systems," *Knowledge-Based Systems*, vol. 120, pp. 87–98, 2017.

[14] Y. L. Zhen, S. G. Ponnambalam, and K. Izui, "Nature inspired algorithms to optimize robot workcell layouts," *Applied Soft Computing*, vol. 49, no. C, pp. 570–589, 2016.

[15] X. Meng and F. Gao, "Basic problems and criteria for synthesis of robotics," *International Journal of Mechanisms and Robotic Systems*, vol. 1, no. 1, pp. 35–48, 2013.

[16] F. Gao, J. Yang, and Q. J. Ge, "Type Synthesis of Parallel Mechanisms Having the Second Class GF Sets and Two Dimensional Rotations," *Journal of Mechanisms and Robotics*, vol. 3, no. 1, pp. 623–632, 2011.

[17] T. Yoshikawa, "Manipulability of robotic mechanisms," *International Journal of Robotics Research*, vol. 4, no. 2, pp. 3–9, 1985.

[18] J. K. Salisbury and J. J. Craig, "Articulated hands: force control and kinematic issues," *International Journal of Robotics Research*, vol. 1, no. 1, pp. 4–17, 1982.

[19] M. H. Abedinnasab, Y. J. Yoon, and H. Zohoor, "Exploiting Higher Kinematic Performance - Using a 4-Legged Redundant PM Rather than Gough-Stewart Platforms," *Serial and Parallel Robot Manipulators - Kinematics, Dynamics, Control and Optimization*, 2012.

[20] B. Zi and S. Qian, *Design, Analysis and Control of Cable-suspended Parallel Robots and Its Applications*, Springer Nature, 2017.

[21] L. Wang, W. Rong, L. Qi, and Z. Qin, "Optimal design of a 6-DOF parallel robot for precise manipulation," in *Proceedings of the 2009 IEEE International Conference on Mechatronics and Automation, ICMA 2009*, pp. 3933–3937, August 2009.

[22] Y. Fang and L.-W. Tsai, "Structure synthesis of a class of 4-DoF and 5-DoF parallel manipulators with identical limb structures," *International Journal of Robotics Research*, vol. 21, no. 9, pp. 799–810, 2002.

[23] W. Xi, B. Chen, L. Ding et al., "Dynamic Parameter Identification for Robot Manipulators with Nonlinear Friction Model," *Transactions of the Chinese Society for Agricultural Machinery*, vol. 48, no. 2, pp. 393–399, 2017.

[24] L. Ding, H. Wu, and Y. Yao, "Chaotic Artificial Bee Colony Algorithm for System Identification of a Small-Scale Unmanned Helicopter," *International Journal of Aerospace Engineering*, vol. 2015, Article ID 801874, 11 pages, 2015.